

## **FRACTURE STRENGTH OF POROUS CERAMICS: STRESS CONCENTRATION VS MINIMUM SOLID AREA MODELS**

F. W. Nyongesa, and B. O. Aduda  
Department of Physics, University of Nairobi  
P.O. Box 30197-00100 Nairobi, Kenya.

**ABSTRACT:-** *In this study, we have reviewed recently published strength-porosity data of porous ceramics, and compared these data with those computed from both the minimum contact solid area (MCA) and the pore stress concentration effect (SCE) models. We observed that the theoretical data (MCA model) matched better the experimental results of ceramics in the low volume fraction porosity range ( $P < 0.25$ ) range, whereas in the volume fraction porosity range ( $P > 0.25$ ), the SCE model better predicts the experimental results.*

### **INTRODUCTION**

The effect of porosity on the fracture strength of porous ceramic materials has been the subject of considerable theoretical as well as experimental investigations [1-13]. Generally, porosity affects the mechanical property of ceramic materials in two ways: Firstly, it reduces the effective cross-sectional (load-bearing) area such that the mechanical property will be dependent on the minimum contact-solid area. The minimum solid (load-bearing) area is the actual sintered or the bond area between particles in the case of stacked particles, and it is the minimum web cross-sectional area between pores in the case of stacked bubbles [1]. Secondly, porosity leads to stress inhomogeneities (stress concentrations) near the pores such that under mechanical loading, the true stress in the material is higher near the pores than at a far distance from them [2].

Accurate prediction of the fracture strength of porous ceramics requires adequate information such as pore shape and orientation to be included, in addition, to pore volume (fraction), as parameters that influence the fracture strength-porosity relationships. The theoretical and experimental studies in the literature can be divided in two main groups: (a) those considering only a pore volume fraction effect on strength and (b) studies which consider a pore structure (size and orientation) effect on the mechanical strength. Two general approaches have thus been developed to explain or predict the fracture strength-porosity relations in ceramic materials. One

approach [1,3], generally called the minimum contact area model (MCA), suggests that the flexural strength ( $\sigma$ ) of ceramics is dependent on the minimum contact solid area. According to this model, the mechanical strength decreases exponentially with increase in volume fraction porosity ( $P$ ) according to Sprigg's [4,14,15]:

$$\sigma = \sigma_0 \exp(-bP) \quad (1)$$

In the above equation,  $\sigma_0$  is the flexural strengths of a fully dense material while  $b$  is an empirical parameter related to the minimum solid area and dependent on the pore structure [3]. Equation (1) was derived on a purely empirical basis (not based on theory) until recently when Andersson [5] analytically derived it. The above equation is applicable when the packing geometry and the shape of the pores remain unchanged as the volume fraction porosity changes [15]. The exact significance of  $b$  is not given in the original work, but it is suggested that  $b$  may be associated with the fabrication technique, and it is related to the proportions of closed and open pores, or to the proportions of continuous solid-phase structure and continuous pore-phase structure [15]. In deriving equation (1), Anderson [5] assumes a large isotropic body within which the pore is contained, and that the remotely applied stress remains invariant. He has shown that  $b$  is a function of pore shape and orientation of the pore with respect to the stress axis and is independent of pore size and it is given by

$$b = 1 + \frac{4(1-\nu^2)}{3\pi} \left[ \frac{E(\alpha) + \pi\alpha}{\alpha E(\alpha)} \right] \text{ for randomly activated pores} \quad (2a)$$

and

$$\frac{2(1-\nu^2)}{\alpha} \left( \frac{2}{\pi} \cos^2 \phi + \frac{\alpha}{E(\alpha)} \sin^2 \phi \right) \text{ for aligned pores} \quad (2b)$$

In the above equation,  $E(\alpha)$  is the complete elliptical integral [5] while  $\alpha$  is the aspect ratio.

Equation (1) does not consider pore interactions and intersections that occur at high porosity and is therefore limited to a porosity range of approximately 40% [5]. Further, this equation does not satisfy the boundary condition  $\sigma = 0$  at  $P = 1$  [7].

The second approach [2], known as the stress concentration effects (SCE) model, suggested that the mechanical property is dependent on pore shape and resulting stress concentration effects. According to this model, the resulting fracture strength-porosity relationship for all ceramic materials can be given by a power equation of the form

$$\sigma = \sigma_o (1 - P)^\eta \quad (3)$$

where, the exponent  $\eta$  is related directly to the pore structure (shape and orientation of the pores with respect to the stress axis) and on the Poisson's ratio of the material via the equation.

$$\eta = 1.21 \left( \frac{z}{x} \right)^{\frac{1}{3}} \sqrt{1 + \left[ \left( \frac{z}{x} \right)^{-2} - 1 \right]} \cos^2 \phi \quad (4)$$

where  $(z/x)$  is the aspect ratio, and  $\phi$  defines the orientation of the pores with respect to the stress direction i.e., the angle between the stress direction and the rotational axis of the spheroids.

The derivation of equation (3) assumes a spheroidal microstructural model, which considers a porous material as a limiting case of two-phase composite consisting of a continuous matrix phase and the inclusion phase (spheroids). Spheroids are defined as objects with regular mathematically definable geometry that have the same surface-to-volume ratio as the real grains/pores. In this model, the pore structure is characterized by three factors: pore distribution, pore shape and orientation of the pores with respect to the stress direction. The mean pore shape is given by the ratio of the rotational ( $z$ ) axes to the minor

( $x$ ) axes and is also called the axial ratio,  $\alpha = (z/x)$  of the spheroids. For  $\alpha = 1$ , the spheroids become spheres and as  $\alpha$  approaches zero, oblate spheroids ( $\alpha < 1$ ) become disc-shaped and prolate spheroids ( $\alpha > 1$ ) become needle-shaped. The orientation factor is defined by  $\cos^2(\phi)$ . The case of random statistical orientation i.e. isotropic materials is obtained by setting  $\cos^2 \phi = 0.33$ . Thus, if enough information about the porosity structure is available (e.g. from quantitative microstructural analysis), then the exponent  $\eta$  can be determined and used in equation (3) to predict the fracture strength of a porous material [6].

Equation (3) is valid in the whole range of porosity for all possible porosity structures and further, it satisfies the boundary condition  $\sigma = 0$  at  $P = 1$  [2]. In the derivation of equation (3), it is assumed that the porosity content and the pore shape have a negligible influence on the Poisson's ratio ( $\nu$ ) i.e., the Poisson's ratio is invariant with porosity.

There is a debate as to which between the MCA and SCE models predicts most accurately the mechanical property-porosity relationship in ceramic materials. For example, Rice [3, 9] has argued against SCE thus: The pore shape can directly effect strength only when at least a few pores are large enough to act as the source of failure i.e., pore shape is only a secondary factor to pore size. Further, in non-dilute or high volume fraction porosity ( $P > 0.05$ ), pore stress concentrations effects are reduced due to interaction between neighbouring pores as pore spacing decreases. Finally, during fracture, crack-pore interactions limit the effects of pore stress concentrations since the stress concentrations are dominated by the crack, and not the pore.

On the other hand, Boccaccini [6] suggested that stress concentration effects mainly from pores play a leading role in all the above three categories. He has indicated that SCE models predict accurately the fracture strength of porous ceramics that fail particularly from pores, i.e., when isolated (large) pores act as fracture origins as was noted too by Kubicki [10]. Further, he has indicated that no interaction between pores should be expected for volume porosity,  $P < 0.4$  if pores are of similar diameter. Thus SCE approach for isolated pores should retain its practical utility for low to intermediate volume fraction porosity ( $P > 0.05$ ). Lastly, on crack-pore interactions, Boccaccini [6] suggests that the stress intensity factor of a crack can be enhanced by a pore for two reasons. First, the crack acts as a fracture flaw, rather than an internal flaw, because it intersects the surface of the pore and, this can double the effective size of the crack.



Secondly, the crack lies in the stress field of the pore and the stress intensity on the crack is increased by the stress concentration of the pore. This idea is supported too by She and Ohji [20] who, propose that crack propagation in porous ceramics is difficult due to crack-pore interaction since, a crack may be arrested when it reaches a pore. Accordingly, fracture depends predominantly on the thermal stress at the neck of the pore and the stress-bearing capability of the neck.

In the present study, our experimental data on porcelain together with recently published data on fracture strength of a number of ceramic materials have been reviewed and compared with predictions of both the MCA and SCE models, to elucidate the range of validity and utility of each of these models in the fracture strength-porosity prediction of these materials. Only materials on which accurate experimental information regarding pore shape was available or which could be inferred from the micrographs given by the original authors were selected.

#### COMPARISON WITH EXPERIMENTAL DATA

The data analyzed in the present work was obtained from our previous experimental work [17] and from literature and includes data on porcelain [16], gypsum [18], alumina [19], sintered glass [18] and uranium dioxide [18]. Table 1 gives the values of the empirical constants  $b$  and calculated from equations (2) and (4) using the information provided by the original authors. In determining  $b$ , the value of  $\nu = 0.23$  was used while in determining  $\eta$ , the value of  $\cos^2\phi = 0.33$  was used (assuming random orientation of pores) together with the values of  $\alpha$  shown in Table 1. Separately, a computer program was run to find the best values of “ $b$ ” and “ $\eta$ ” corresponding to the best fit of equations (1) and (3) to the experimental data of each material respectively. These values are also shown in Table 1.

It is observed from Table 1 that the calculated  $\eta$  values from equation (4) lie between 2.0 and 5.5 (Table 1.) while the values that give the best fit to the experimental data lie between 2 and 3.45. Comparatively, for each material, the calculated value is very close to the value that gives the best fit except for gypsum. The high values of  $\eta$  could be associated with the presence of extreme cases of pore shapes (e.g. extreme prolate, oblate or for oriented pores) [13], introduced possibly by the method of preparation. For example, extrusion is more likely to introduce pores (whose axes are parallel to the direction of stress), whereas, uniaxial pressing would introduce oblate pores. Pores of such morphologies should result in increased stress concentration effects.

On the other hand, the values of  $b$  obtained in this study range between 2.08 and 3.60. These values are in the range (2.0 - 9.0) for most ceramics [9]. The value of  $b$  is also associated with different processing techniques [15] since this gives rise to different pore structures. Thus, more densely packed materials have higher values of  $b$ . It was further observed that the calculated values of  $b$  and  $\eta$  are in most cases higher than the best fit values. Previous results [22] indicate that the single “effective”  $\alpha$  values (used to calculate  $b$  and  $\eta$  in this case), obtained from stereological equations, are usually much higher, resulting in calculated higher values of the fitting parameters. Stereological equations overestimate the value of the ‘effective’ aspect ratio.

Figures 1-6 show the comparison between the experimental data of the various ceramic samples investigated in this study with the predictions based on both the MCA model (Equation (1)) and the SCE model (Equation (3)). The equations were fitted using the best fit parameters “ $b$ ” and “ $\eta$ ” shown in Table 1. A clear observation from all the figures indicates that at low volume porosity ( $P < 0.20$ ), the MCA model predicts better

**Table 1. Summary of the materials used together with calculated values of empirical parameters based on Equations (1) and (3)**

Material	Fitting parameters				
	$b$	$\eta$	$\alpha$	$b^*$	$\eta^*$
Porcelain [Ref 17]	3.3	-	0.25	3.6	3.5
Porcelain [Ref 16]	3.2	-	0.15	2.8	2.5
Gypsum [Ref 18]	-	5.5	-	2.1	2
Alumina with spherical pores [Ref 19]	3.5	2.2	0.8	2.5	2.5
Sintered glass (spherical pores) [Ref 18]	-	2	-	3.1	2.5
Uranium dioxide (spherical pores) [Ref 18]	3.7	2.7	0.6	2.8	2

\* best fit values obtained using a computer program

the strength-porosity relationship in most ceramic materials compared to the SCE model. This observation supports the idea of Rice [7], that porosity-property dependence of materials with dilute (isolated) porosity is dependent on the minimum solid area since in this low porosity range, most pores are closed and isolated as evidenced by SEM micrograph of Fig. (7). Thus in such materials, the value of  $\alpha \rightarrow 1$ , yielding low values of  $\eta$  according to equation (3). Contrary to suggestions by

Boccaccini [6] and Kubicki [10], at low volume fraction porosity, isolated (closed) pores tend not to have sharp edges that may enhance stress concentrations. Further, in this porosity range, crack propagation (during fracture) may be difficult since the crack (if any) may be arrested by a pore and as such, fracture will depend predominantly on the stress bearing capability of the neck (actual load bearing area).

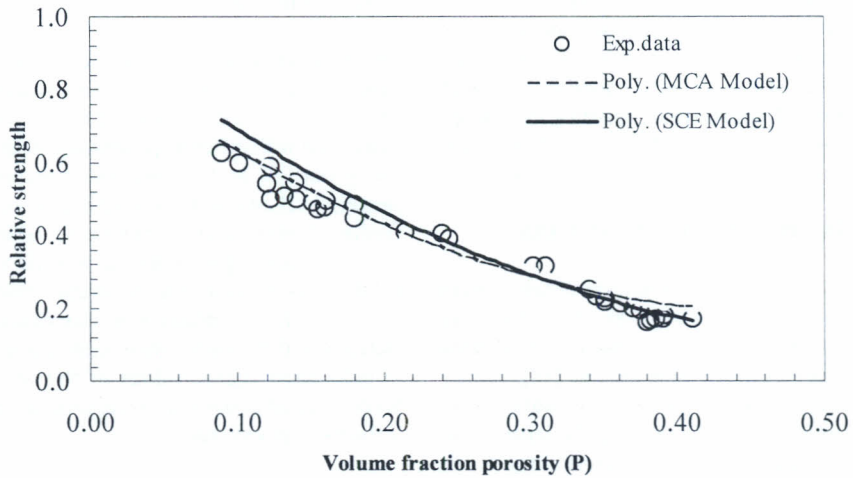


Figure 1. Comparison of experimental data of porcelain [17] with calculated values of flexural strength in based on SCE and MCA models

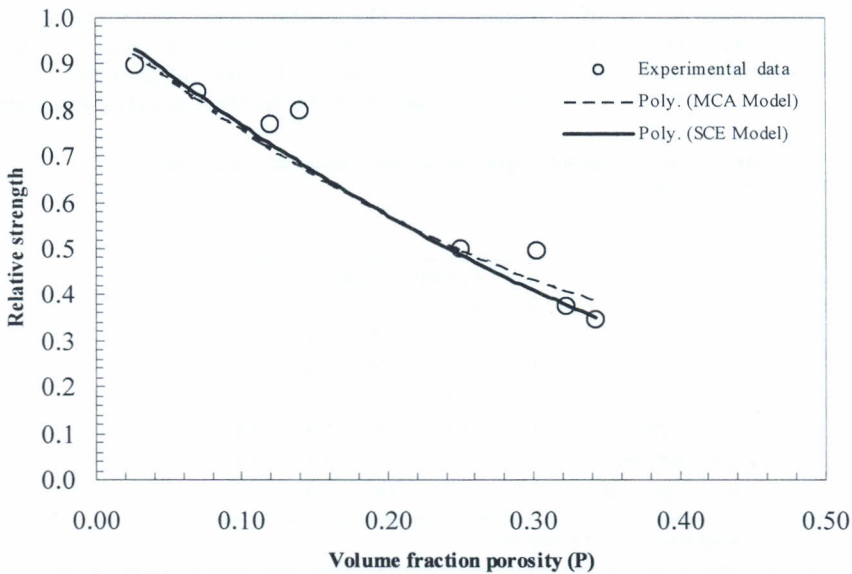


Figure 2. Comparison of experimental data of porcelain [16] with calculated values of flexural strength based on SCE and MCA models

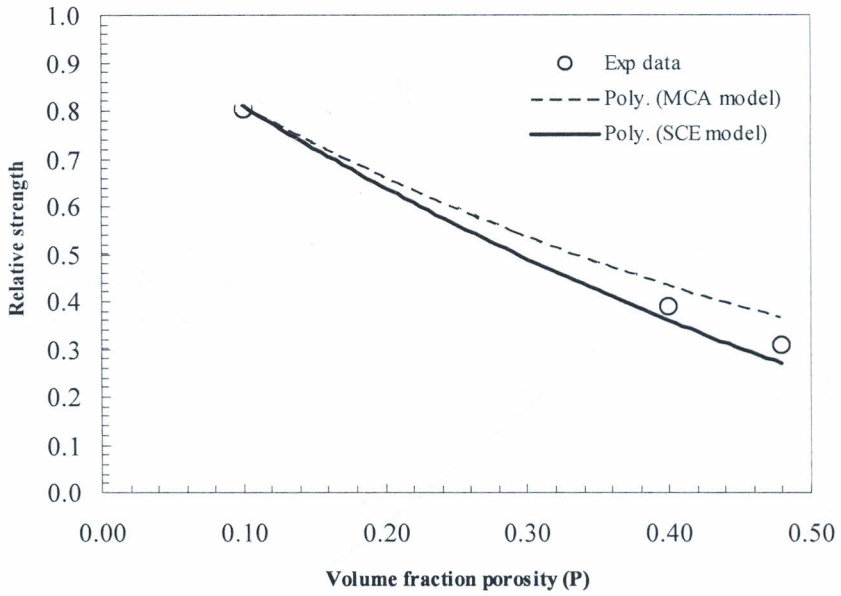


Figure 3. Comparison of experimental data of Gypsum [18] with calculated values of flexural strength based on SCE and MCA models

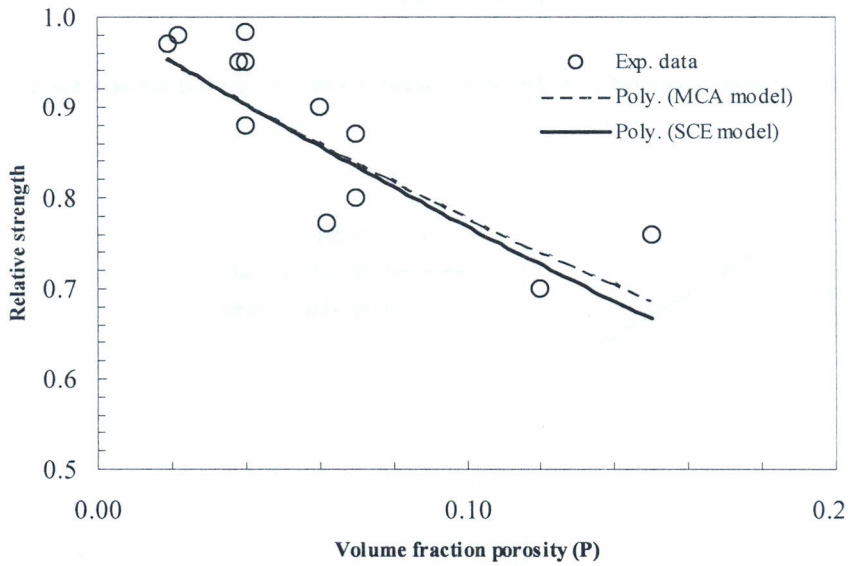


Figure 4. Comparison of experimental data in alumina [19] with calculated values of flexural strength based on SCE and MCA models

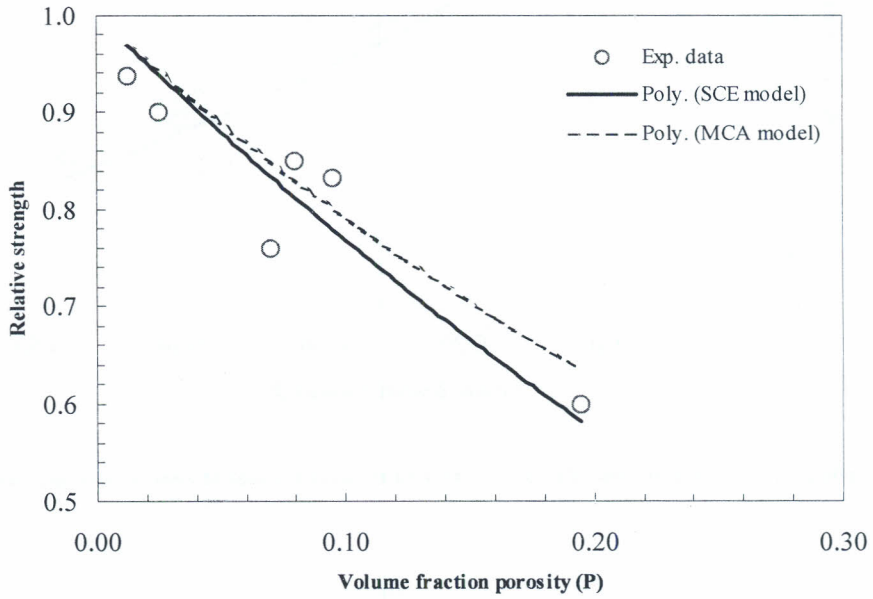


Figure 5. Comparison of experimental data of sintered glass [18] with calculated values of flexural strength based on SCE and MCA models

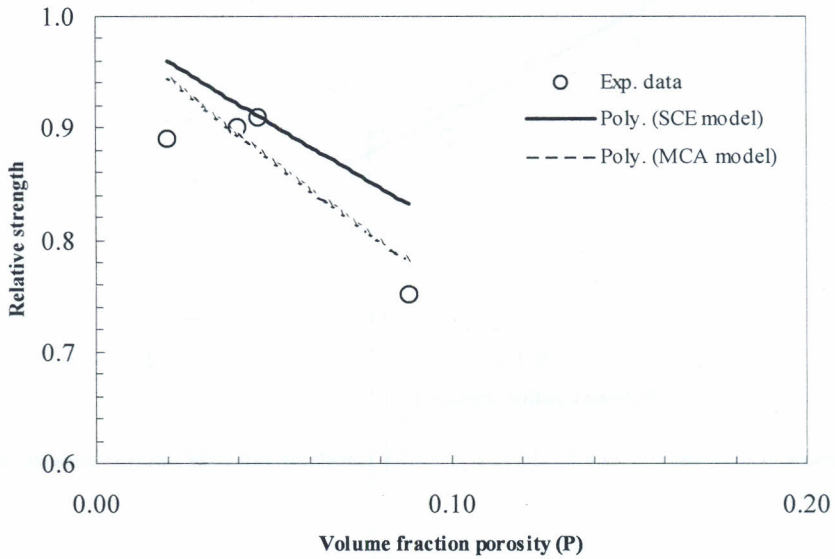


Figure 6. Comparison of experimental data of uranium dioxide [18] with calculated values of flexural strength based on SCE and MCA models



In the intermediate volume porosity range,  $0.20 \leq P \leq 0.30$ , both models predict a similar variation of strength-porosity relationship. In this porosity range, as pore sizes increase, pores start to interact with the nearest neighbours. Consequently, pores depart from spherical shape as porosity increases. This observation was noted by Aduda and Boccaccini [21] in their Fig. 4, from which they gave an empirical correlation between the aspect ratio  $\alpha = z/x$ , and porosity ( $P$ ) as:

$$\alpha(P) = 1 - AP \quad (5)$$

where  $A$  is an empirical constant.

We therefore expect the  $b$  values to decrease since  $\alpha \rightarrow 0$ , or becomes  $>1$  while  $\eta$  values increases. Consequently, pore interaction reduces the minimum solid contact area between the solid phases but enhances the stress

concentration from the pores. For this reason, the MCA starts losing its range of applicability while the SCE starts to show dominance.

At high volume porosity range, ( $P > 0.30$ ), the SCE model gives a better prediction of the experimental data. This is because, in this porosity range, pores are interconnected. SEM analysis (Fig. 7) reveals pore interaction at volume fraction porosity ( $P > 30$ ) for porcelain samples from ref. [22]. We therefore expect the effect of both pore-pore interactions as well as pore-crack interactions to come into play as suggested by Boccaccini [6]. The fact that the exponential relationship becomes invalid at high pore fractions is therefore not surprising. Accordingly, the pore may enhance the stress intensity factor of the crack by increasing the effective size of the crack especially if the crack (which is parallel to the stress direction) intersects the surface of a prolate shaped pore.

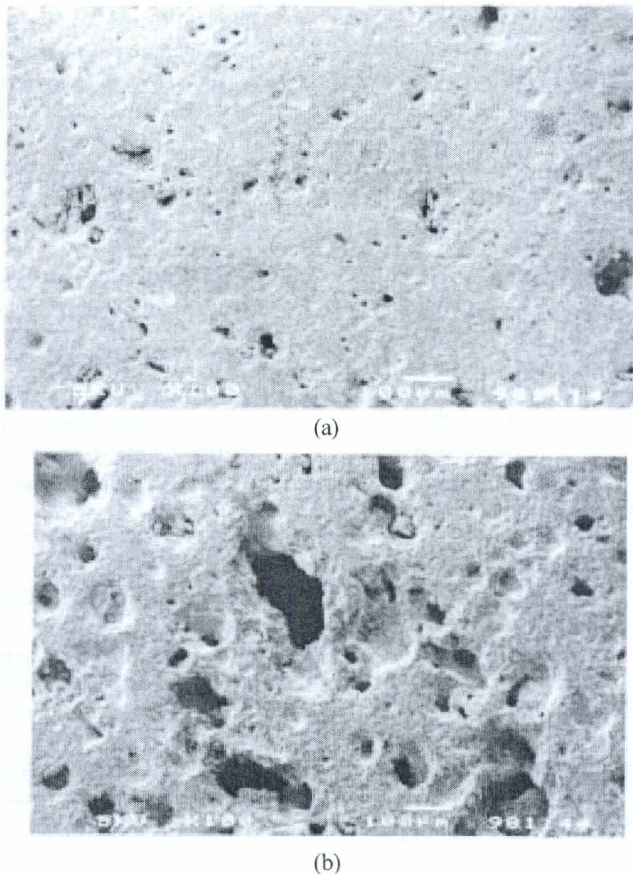


**Figure 7. SEM micrograph of polished section of porcelain sample (a) Showing isolated closed pores ( $P = 0.18$ ) and (b) showing interconnected pores ( $P = 0.36$ )**

It is important to note that in sintered ceramic materials, the shape, and hence the aspect ratio, changes with the porosity level [23]. For this reason, we would recommend an analysis of the fracture strength-porosity relationship on a point-by-point basis, thus determining at each porosity level, the value of the axial ratio which provides the best fit as opposed to using a single "effective" aspect ratio. A number of authors [21,22] have successfully applied this concept in the elastic property versus porosity data in various ceramic materials.

### CONCLUSIONS

The present study was undertaken to verify the prediction capability of the SCE and the MCA models proposed for the fracture strength-porosity correlation in porous ceramics. It can be concluded that the MCA model have a better prediction capability in the low to intermediate volume fraction porosity range ( $P \leq 0.25$ ) while the SCE model predicts better the fracture strength-porosity relationship of ceramics in the intermediate to high porosity range ( $P \geq 0.25$ ).

### ACKNOWLEDGEMENTS

One of the authors (FWN) wishes to thank the Germany Academic Exchange (DAAD) for award of the fellowship. Both authors sincerely acknowledge the assistance of Mr. Chimtawi of the International Centre for Insect Physiology and Ecology (ICIPE) with taking the SEM micrographs.

### REFERENCES

1. RICE R. W., (1996a). Evaluation and Extension of Physical Property-Porosity Models Based on Minimum Solid Area, *Journal of Materials Science* **31**, 102-118.
2. BOCCACCINI A. R., ONDRACEK G., MAZILU P., WINDELBERG D., (1993). On the Porosity Dependence of the Fracture Strength of Ceramics in 'Third Euro-Ceramics, Engineering Ceramics', Edited by DURAN P. and FERNANDEZ J.F., **3**, 895-900.
3. RICE R. W., (1993a). Evaluating Porosity Parameters for Porosity-Property Relations, *Journal of American Ceramic Society*, **76** [7], 1801-1808.
4. KNUDSEN F. P., (1959). Dependence of Mechanical Strength of Brittle Polycrystalline Specimens on Porosity and Grain Size, *Journal of American Ceramic*

- Society, **42** [8], 366-387.
5. ANDERSSON C. A., (1996). Derivation of the Exponential Relation for the Effect of Ellipsoidal Porosity on Elastic Modulus, *Journal of American Ceramic Society*, **79** [8], 2181-84.
6. BOCCACCINI A. R., (1998). Influence of Stress Concentrations on Mechanical Property- Porosity Correlation in Porous Materials, *Journal of Material Science Letters*, **17**, 1273-75.
7. RICE R. W. (1997). Limitations of Pore-Stress Concentrations on the Mechanical Properties of Porous Materials, *Journal of Materials Science*, **32**, 4731-4736.
8. RICE R. W., (1993b). Comparison of Stress Concentration versus Minimum Solid Area Based Mechanical Property-Porosity Relations, *Journal of Materials Science*, **28**, 2187-2190.
9. RICE R. W., (1996b). Comparison of Physical Property-Porosity Behaviour with Minimum Solid Area, *Journal of Materials Science*, **31**, 1509-1528.
10. KUBICKI B., (1995). Stress Concentration at Pores in Sintered Materials, *Powder Metallurgy*, **38** [4], 295-98.
11. HASSELMAN D. P. H. and FULRATH R. M., (1967). Micromechanical Stress Concentration in Two Phase Brittle-Matrix Ceramic Composites, *Journal of American Ceramic Society*, **50** [8], 399-404.
12. BOCCACCINI A. R., (1997). Comment on Dependence of Ceramic Fracture Properties on Porosity, *Journal of Materials Science Letters*, **16**, 683-684.
13. ARATO P., (1996). Comment on Dependence of Ceramics Fracture Properties on Porosity. *Journal of Materials Science Letters*, **15**, 32-33.
14. DUCKWORTH W., (1953). Discussions of Ryskhewitch Paper by Winston Duckworth, *Journal of American Ceramic Society*, **36**, 68.
15. SHE J. and OHJI T., (2002). Thermal Shock Behaviour of Porous Silicon Carbide Ceramics. *Journal of American Ceramic Society*, **85**[8], 2125-27.
16. BOCCACCINI N. and BOCCACCINI A. R., (1997). Dependence of Ultrasonic Velocity on Porosity and Pore shape in Sintered Materials, *Journal of*



- Nondestructive Evaluation, **16** [4], 187-192.
17. NYONGESA F.W., (2000). Influence of Sintering Temperature and Composition on Physio-mechanical Properties of Kenyan Triaxial Porcelain, Ph.D Thesis, (University of Nairobi).
18. BOCCACCINI A. R., (1994). Comment on “Dependence of Ceramic Fracture Properties on Porosity”, Journal of Material Science Letters, **13**, 1035-37.
19. COBLE R. L. and KINGERY W. D., (1956). Effect of Porosity on Physical Properties of Sintered Alumina, Journal of American Ceramic Society, **39** [11], 377-85.
20. SPRIGGS R. S., (1961). Expression for Effect of Porosity on Elastic Moduli of Polycrystalline Refractory Materials, Particularly Aluminum Oxide, Journal of American Ceramic Society, **44** [12], 628-29.
21. ADUDA B. O. and BOCCACCINI A. R., (2003). Velocity of elastic waves in porous ceramic materials: Influence of pore structure. British Ceramic Transactions, **102**[3], 103-108
22. ADUDA B. O. and NYONGESA F. W., (1999). The role of Aspect Ratio in Elastic Modulus-Porosity Relationship of Triaxial Porcelain, British Ceramic Transactions, **99**[5], 206-211.
23. MARTIN L. P., DADON D. and ROSEN M., (1996). Evaluation of Ultrasonically Determined Elastic-Porosity Relation in Zinc Oxide, Journal of American Ceramic Society, **79** [5], 1281-89.